Stable dynamics in a Greenland tidewater glacier over 26 years despite reported thinning

Suzanne L. BEVAN,[1] Tavi MURRAY,[1] Adrian J. LUCKMAN,[1] Edward HANNA,[2] Philippe HUYBRECHTS[3]

[1]*Geography Department, College of Science, Swansea University, Swansea, UK*
E-mail: s.l.bevan@swansea.ac.uk
[2]*Department of Geography, University of Sheffield, Sheffield, UK*
[3]*Earth System Sciences and Departement Geografie, Vrije Universiteit Brussel, Brussels, Belgium*

ABSTRACT. Daugaard Jensen Gletscher, Greenland, is a large tidewater glacier terminating in the northwest corner of the Scoresby Sund fjords. We present a time series of surface flow speeds spanning 1985–2010 based on feature tracking of satellite images. The time series confirms that flow speeds remained stable and reveals a persistent summer acceleration of up to 10% over the lower 10 km of the glacier. The front of the 6 km floating tongue fluctuates by little more than the average size of calved icebergs, ~1 km. While we are unable to detect any imbalance between ice discharge and surface mass balance within our error estimates, observations suggest that the region is losing mass and experiencing decreases in surface elevation. We conclude that as flow speeds and surface mass balance have remained steady since 1985, the shift from balance to imbalance, leading to elevation decrease, must have occurred prior to this date. As for other stable Greenland tidewater glaciers, the seasonal melt cycle is the dominant influence on flow velocity variation but, if the apparent current thinning rates continue, there is potential for the grounding line to retreat, for calving rates to increase and for the glacier to accelerate.

INTRODUCTION

Daugaard Jensen Gletscher is a tidewater-terminating outlet glacier covering an estimated 4% of the Greenland ice sheet, which discharges into the northwest corner of the Scoresby Sund fjord system in eastern Greenland. We investigate whether recent changes in the dynamics and mass balance of this sector of the Greenland ice sheet are reflected in the behaviour of this particular glacier. Since 2002, gravity field observations made by the Gravity Recovery and Climate Experiment (GRACE) have shown that the Greenland ice sheet has been losing mass (Velicogna and Wahr, 2005) at an increasing rate (Chen and others, 2006; Wouters and others, 2008; Velicogna, 2009), with mass losses first appearing in the south and later also in the northwest (Khan and others, 2010). Progressive improvements in the ability to spatially resolve the mass loss signal show the sign, magnitude and temporal evolution to be dependent on drainage basin and altitude (Luthcke and others, 2006; Wouters and others, 2008; Schrama and Wouters, 2011). The total mass loss of ~1500 Gt between 2000 and 2008 appeared to be equally partitioned between surface processes and ice dynamics (Van den Broeke and others, 2009). Modelling studies have shown surface mass balance (SMB) to be only slightly negative over various time periods since the early 1990s, with increases in run-off largely compensated for by increases in accumulation (Hanna and others, 2005, 2008; Box and others, 2006; Wake and others, 2009). The SMB variability is focused in the ablation zone, which is consistent with observed elevation decreases at lower altitudes (Krabill and others, 2004; Pritchard and others, 2009). The significance of ice dynamic changes in mass loss is indicated by the inability to account for either mass or volume loss by changes in SMB alone (Pritchard and others, 2009; Van den Broeke and others, 2009). Rates of volume loss are also larger over fast-flowing compared with slow-flowing regions.

Between 1992 and 2009 there was a steady increase in the total Greenland ice discharge of $9.0 \pm 1.0\,\mathrm{Gt\,a^{-2}}$ (Rignot and others, 2011). However, within this trend there was much spatial and temporal variability with widespread glacier acceleration between 1996 and 2000 south of 66° N, appearing as far north as 70° N by 2005 (Rignot and Kanagaratnam, 2006). During the last 15 years three major tidewater glaciers have exhibited remarkable accelerations in flow speed: first Jakobshavn Isbræ in the west (Joughin and others, 2004; Luckman and Murray, 2005) and then Helheim and Kangerdlugssuaq glaciers in the southeast (Howat and others, 2005; Luckman and others, 2006), the latter pair subsequently decelerating (Howat and others, 2007). These three glaciers also retreated significantly, a trend that has been a feature of many tidewater glaciers, particularly in southeast Greenland, for the last decade (Moon and Joughin, 2008; Murray and others, 2010). The ocean probably played a significant part in driving the retreat of both the southeastern glaciers (Murray and others, 2010; Christoffersen and others, 2011) and Jakobshavn Isbræ (Holland and others, 2008; Motyka and others, 2011) by reducing the amount of ice melange in the fjord (Amundson and others, 2010), by increasing calving-front (Nick and others, 2009) or basal melt rates (Holland and others, 2008) or by a combination of these factors.

Estimates of mass loss based on flux-balance methods and GRACE gravity field observations are in general agreement (Van den Broeke and others, 2009; Rignot and others, 2011), but in places there has been some difficulty in reconciling volume losses with relatively stable flow speeds. For example, elevation decreases were observed during the 1990s on Kangerdlugssuaq Gletscher during a period of relative stability in flow speeds (Thomas and others, 2000; Luckman and others, 2006). Also, in the northwest, glacier surface elevations were lowering but there was a lack of

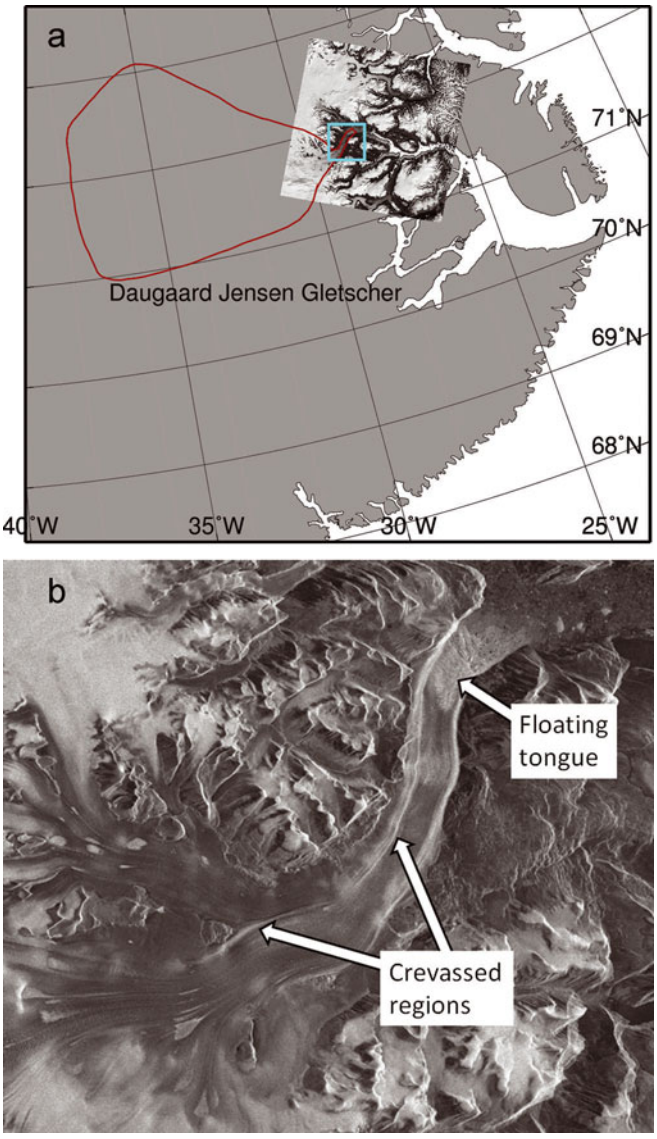

Fig. 1. (a) Location of Daugaard Jensen Gletscher. The image overlain is a Landsat image. The cyan box shows the region covered in Figure 2 and the red outline shows the catchment boundary. (b) Subsection of an ERS-1 SAR image acquired on 17 March 1993. The image covers approximately 60 km × 60 km and is in slant-range and azimuth coordinates. Heavily crevassed regions, such as the floating tongue and marginal shear regions, enhance the backscatter and are visible as bright regions.

dynamic change during the same period, implying that the thinning in the last decade (Pritchard and others, 2009) has been ongoing since some time prior to the start of the velocity measurement record in 1996 (Rignot and Kanagaratnam, 2006).

Daugaard Jensen Gletscher (71.9° N, 28.5° W) is in the basin group immediately to the north of the group showing the greatest mass loss and well within the region exhibiting significant although decelerating annual losses (Wouters and others, 2008; Schrama and Wouters, 2011). The glacier has a short floating tongue of ~6 km and an estimated thickness at the grounding line of ~500 m (Stearns and others, 2005). Remotely sensed velocities in 2000 matched those measured in situ in 1968 (Reeh and Olesen, 1986), and the frontal position had also remained the same (Stearns and others, 2005).

Estimates based on comparisons between measured and balance fluxes suggest that Daugaard Jensen Gletscher had a neutral mass balance in 1996 (Rignot and others, 2004) and a slightly negative mass balance in 2000 (Stearns and others, 2005). However, in keeping with much of the Greenland ice sheet, the lower elevations of Daugaard Jensen Gletscher now appear to be thinning at ~0.3 m a^{-1}. Estimates include a local thinning rate 100 km up-glacier of 0.281 ± 0.204 m a^{-1} over approximately the last 100 years (Hamilton and Whillans, 2002) and, based on Ice, Cloud and land Elevation Satellite (ICESat) data, a dynamic thinning of 0.3 m a^{-1} and a surface mass-balance thinning of 0.1 m a^{-1} between 2003 and 2007 at an altitude of 2000 m within the catchment (Pritchard and others, 2009).

In this paper we derive a 26 year time series of surface velocities and frontal positions spanning the period 1985–2011 and identify the dynamic characteristics and calving behaviour of the glacier. We then compare an estimate of the mean balance flux for the same period based on modelled SMB, in an attempt to account for the apparent loss in mass and thickness in the lower catchment region.

METHOD

Catchment and grounding line

Figure 1a shows the location of Daugaard Jensen Gletscher overlain with a Landsat image. The catchment boundary was delineated by tracing flowlines upstream from the glacier terminus following the method of Costa-Cabral and Burges (1994). Flow directions were derived from smoothed fields of gravitational driving stress (GDS) (Le Brocq and others, 2006). The GDSs were based on a digital elevation model (DEM) and an ice-thickness grid of 5 km resolution (Bamber and others, 2001). The GDS fields were computed at 1 km resolution and linearly smoothed over a distance equivalent to 20 times the ice thickness. The selection of start points at the glacier terminus was restricted to locations covered by the DEM and guided by visual inspection of the ice margins and velocity distribution.

Following Stearns and others (2005) we assume that the grounding line is located close to where the crevasse pattern on the surface of the glacier changes: as the tongue goes afloat the crevasses become wider. The crevasses are clear in winter synthetic aperture radar (SAR) images (Fig. 1b) where microwaves are able to penetrate dry snow cover and backscatter is high from crevasses, particularly those oriented normal to the incidence angle of the radar.

Intensity feature tracking to measure surface velocities

A time series of surface velocities for Daugaard Jensen Gletscher was generated by applying intensity feature tracking to European Remote-sensing Satellite 1 (ERS-1), ERS-2 and Envisat advanced SAR (ASAR), Landsat-5 Thematic Mapper (TM) band 4 and Landsat-7 Enhanced TM Plus (ETM+) band 8 image pairs. Before tracking, the Landsat-5 and -7 images were resampled using a quadratic interpolation from 30 to 20 m and from 15 to 10 m, respectively, and re-projected to the polar stereographic coordinate system. The SAR images were tracked in slant-range and azimuth geometry after 1 × 5 multi-looking to a pixel size of ~8 m × 20 m. This ratio of multi-looking results in approximately square pixels when the displacements are converted to ground range.

The use of feature tracking to measure glacier flow was first demonstrated on optical satellite images (Scambos and others, 1992) and has since been applied successfully to SAR satellite images (Lucchitta and others, 1995; Luckman and others, 2002, 2003; Strozzi and others, 2002; Pritchard and others, 2005). The method relies on large-scale patterns in image intensity being correlated between successive images. A two-dimensional (2-D) array of offsets is produced between a small patch of intensities from the first image and an equivalent patch in the second image. When the range and azimuth offsets between the two patches match the actual local displacement between the two images, there will be a peak in the intensity cross-correlation. A 2-D second-order polynomial is fitted to the array of correlation values, enabling the position of the peak to be determined with sub-pixel accuracy. By repeating the procedure across the scene, a complete field of local offsets is produced. Here patch sizes of 1000 m × 1000 m were used over search areas of 3200 m × 3200 m for the SAR images, for which the temporal separation was 35 days, and 800 m × 800 m over search areas of 1760 m × 1760 m or 2720 m × 2720 m for the Landsat images, where the temporal separation was either 16 or 32 days, respectively. A spatial sampling for the patches was selected such that offset fields were produced at a resolution of 40 m for all image types.

All offset fields were corrected to a background reference such that non-moving areas were set to zero. The resulting offset fields were filtered according to the signal-to-noise ratio of the correlation peak, and SAR image displacements were converted from slant range and azimuth to surface parallel using orbit data and the Advanced Spaceborne Thermal Emission and Reflection Radiometer (ASTER) global DEM (GDEM). The final velocity fields were then filtered by expected downslope flow direction (Luckman and others, 2006).

For both SAR and optical data it is necessary to track between pairs of images acquired on the same satellite track in order to preserve the solar and viewing geometries. In total, 135 pairs of Landsat images with temporal separations of either 16 or 32 days were successfully tracked, as well as 53 pairs of SAR images with temporal separations of 35 days.

The errors associated with determination of surface velocity using feature tracking include random errors associated with determination of the 2-D offset and systematic errors associated with re-projection and geolocation. Co-registration of patches with a precision of 1/10 (Gray and others, 2001) to 1/20 (Strozzi and others, 2002) of a pixel is possible, so the errors associated with determining the offsets are, at the most, 0.2 m d^{-1} for tracking of Landsat-5 images over 16 days, and less for the other image pairs. Errors introduced during subsequent processing are estimated by measuring the mean displacement over a stationary point close to the front of the glacier. For the Landsat-5 images the mean displacement at this point was 0.28 m d^{-1}, for Landsat-7 images it was 0.09 m d^{-1} and for the SAR images it was 0.22 m d^{-1}. Combining the above errors as independent error sources results in a maximum estimated error of 0.34 m d^{-1}.

Frontal positions

Frontal positions were digitized manually on each Landsat and SAR image including those unsuitable for tracking. In addition, a set of Envisat ASAR Wide Swath Mode (WSM) images, covering the ice front between December 2006 and January 2011, were geocoded and used to locate the front position. The intersection points of the digitized fronts with a centre-line profile were used as single-point indicators of midfront position. In total, 214 frontal positions were located on Landsat, 87 on image mode SAR and 658 on WSM SAR images.

Errors in frontal locations can arise as a result of geolocation error and also depend on the precision with which the fronts are digitized. The errors are likely to depend on image type and resolution. Relative errors were estimated by digitizing a section of fjord wall adjacent to the frontal zone. For 30 randomly selected Landsat-5 TM images the standard deviation of the intersection of these vectors with a profile drawn at right angles to the wall was 76 m. The Landsat-7 ETM+ images are of a higher resolution and are more accurately geocoded and are therefore expected to have smaller relative errors. For 30 randomly selected image-mode SAR scenes the corresponding standard deviation was 49 m. The ASAR WSM images are of a coarser resolution than the other images used (100 m), and the frontal positions will therefore have greater random errors. For 90 randomly selected WSM images the standard deviation of the measured position of the fjord wall was 227 m.

Balance fluxes

In order to determine whether Daugaard Jensen Gletscher discharge fluxes are in balance with net accumulation and ablation, modelled SMB values were totalled for each calendar year from 1985 to 2010 over the glacier catchment area.

Runoff, snow accumulation and SMB were modelled for the whole of Greenland using a modified monthly version of the Janssens and Huybrechts (2000) runoff/retention scheme. This model uses monthly average near-surface (2 m) air temperature, based on European Centre for Medium-Range Weather Forecasts (ECMWF) meteorological reanalysis and corrected for Greenland orography errors (Hanna and others, 2005, 2008), to calculate positive degree-days. These parameters are then used together with degree-day factors of 2.7 mm $°C^{-1}$ d^{-1} (snow) and 7.2 mm $°C^{-1}$ d^{-1} (ice) and an assumed variability of 6 hourly temperatures about the monthly mean – these factors were tuned against previous Greenland field data referenced in Janssens and Huybrechts (2000) – to calculate melt. Monthly precipitation is also used as an input to the model; this too is based on ECMWF reanalysis net precipitation (precipitation minus evaporation and sublimation) data that have been regionally calibrated against the corrected precipitation map of Bales and others (2009) to remove spatial biases in the ECMWF precipitation fields. Not all the modelled melt runs off: some is retained in the snowpack as capillary water and partly refreezes as superimposed ice in the surface layer, although obviously some of this superimposed ice subsequently melts. Modelled melt has to reach a certain fraction, typically 0.6, of annual precipitation before surface meltwater runoff is initiated, so the model implicitly includes consideration of the ice–albedo feedback. This Greenland runoff/SMB model set-up has been specially adapted for use with downscaled/gridded meteorological analysis fields and has been used widely in previous studies (e.g. Hanna and others, 2005, 2008, 2009; Sundal and others, 2009, 2011; Murray and others, 2010). The SMB model output data used in this study have been produced on a 5 km × 5 km grid in line with the downscaled meteorological data, based on an

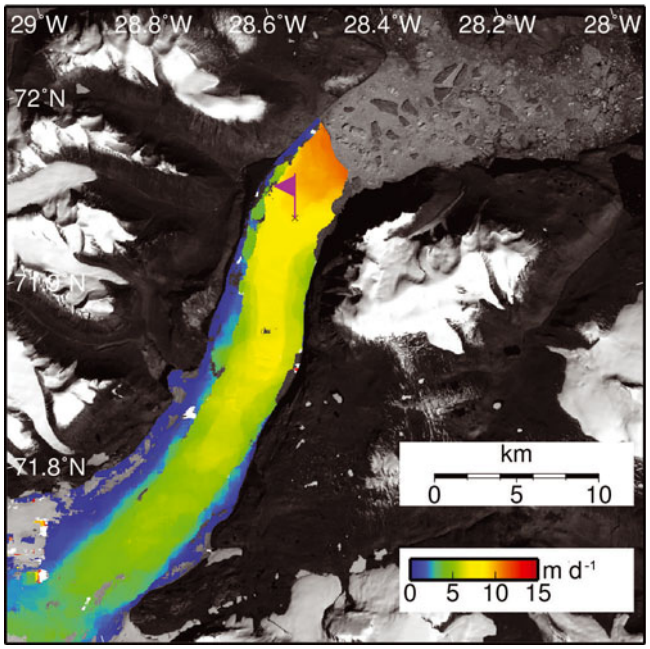

Fig. 2. Results of feature tracking between Landsat-5 images acquired on 18 July and 19 August 1986. The flag marks the location of the extraction point for the time series of velocities presented in Figures 3 and 4.

accurate DEM for Greenland (Ekholm, 1996; Janssens and Huybrechts, 2000), and can be related to climatic fluctuations at the local-to-regional (drainage basin) scale.

RESULTS AND DISCUSSION

Velocities

Using the Landsat images it is possible to obtain an almost complete spatial coverage of velocity estimates over the lower 30 km of the glacier. Figure 2 shows an example of the flow-speed distribution across the glacier obtained by feature tracking between Landsat-5 images acquired on 18 July and 19 August 1986. Not all tracked pairs produced as complete a coverage as this example and the Landsat tracking generally resulted in a better spatial coverage than the SAR tracking. However, the SAR tracking allowed velocities to be derived under cloudy conditions and during the polar night. In this example the speed at the terminus was 11.2 ± 0.3 m d^{-1}, falling to 3.0 ± 0.3 m d^{-1} at 45 km up-glacier.

In total, 188 flow-speed estimates were extracted from the tracking results for a point in the centre of the glacier (marked by the flag in Fig. 2) 5 km upstream of the front close to the point at which the tongue appears to unground, as revealed by increased surface crevassing. The complete time series is shown in Figure 3b. The minimum speed of 7.4 ± 0.3 m d^{-1} occurred in June 1990 and the maximum of 10.0 ± 0.3 m d^{-1} occurred in June 2007. Apart from a few measurements in 2006 and 2007, surface speeds appear to have remained stable throughout the period. There is a consistent seasonal cycle in speed which is easier to identify in Figure 4, in which the last 6 years of measurements are expanded. The time-span covered by these velocity measurements includes periods of cool (1985–95) and then increasing (after 1995) surface air temperatures as reported by coastal weather stations to the north and to the south of Daugaard Jensen Gletscher (Chylek and others, 2006). There is thus no evidence here that variations in surface air temperatures on the lower reaches of the glacier are having a discernible impact on glacier dynamics over multi-annual timescales.

Apparent differences between measurements plotted at the same time but from different data sources will be a combination of measurement error and different temporal averaging periods: 16, 32 or 35 days. Twice-daily in situ velocity measurements on the glacier in 1968 and 1972 (Reeh and Olesen, 1986) revealed short-period (2–10 day) speed increases of 10–15%, probably related to changes in the subglacial drainage system, and one instance of an acceleration of 50% over a 12–18 hour period coinciding with a lake drainage event 17 km upstream of the terminus. These short-period velocity changes can clearly result in discrepancies in velocity estimates based on longer temporal averaging periods when the periods do not exactly overlap.

To reveal the spatial distribution of summertime acceleration of glacier flow, all July Landsat-derived speeds were averaged together and divided by the average of all Landsat-derived speeds. This method is likely to underestimate the maximum acceleration with respect to the annual mean because velocities can only be measured with Landsat images between March and October at this latitude.

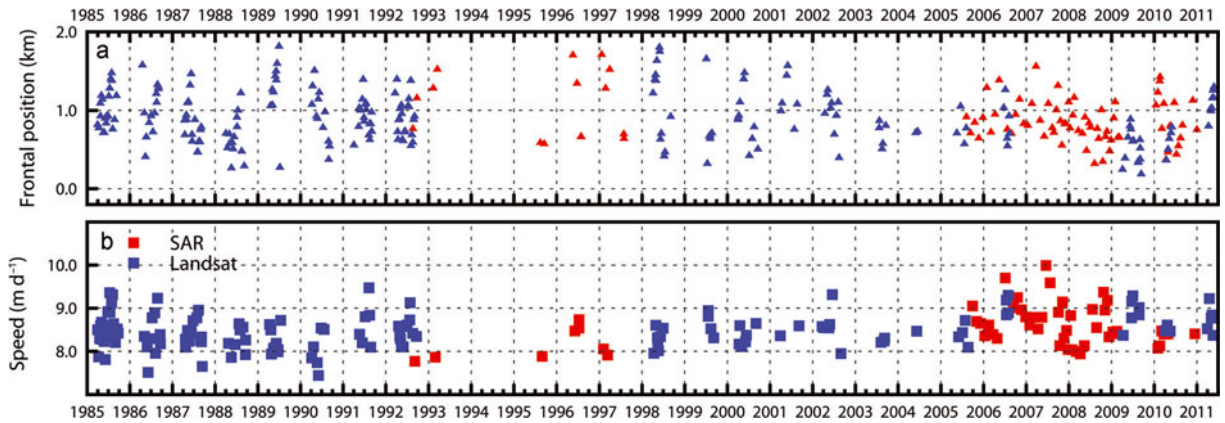

Fig. 3. (a) Centre front position relative to most retreated position based on Landsat images and ERS-1 and -2 SAR and Envisat ASAR image mode scenes. (b) Complete time series of velocity magnitudes extracted from a point 5 km upstream of the glacier front (see flag in Fig. 2). In both (a) and (b) Landsat measurements are in blue and SAR measurements are in red.

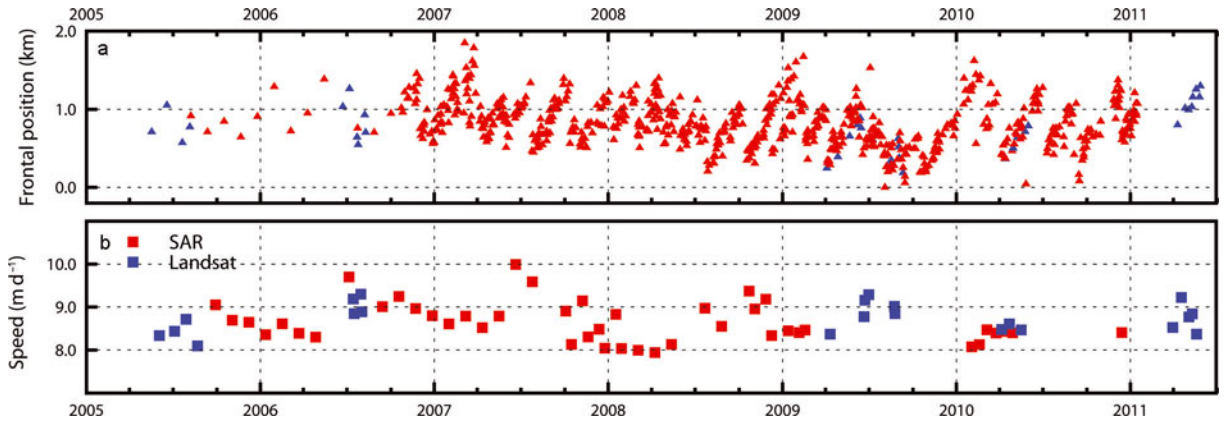

Fig. 4. (a) Centre front position relative to most retreated position based on Landsat images (blue) and ERS-1 and -2 SAR and Envisat ASAR image and WSM scenes (red). (b) 2005–10 subset of velocity magnitudes from Figure 3.

However, the improved spatial coverage of velocity measurements based on Landsat, compared with SAR, results in a more even distribution of frequency of observations per pixel and, therefore, a spatially smocother representation of the signal.

Figure 5, with the grounding line as identifiable in SAR images (e.g. Fig. 1b) shown in green, shows July accelerations of up to 10% close to the front. This magnitude of seasonal acceleration is typical of stable tidewater glaciers in Greenland (Joughin and others, 2008; Andersen and others, 2010; Howat and others, 2010) where the seasonal cycle is governed by meltwater input to the bed. For glaciers where terminus conditions dictate the flow speed, such as Jakobshavn Isbræ on the western coast of Greenland, the magnitude of acceleration can be much higher (Joughin and others, 2008). Upstream of the grounding line, the acceleration factor increases in the along-flow direction where meltwater production is greatest and where it can accumulate from upstream. The acceleration is also greater along a flowline originating from a nunatak. The glacier is heavily crevassed along the region of this flowline, as can be seen in Figure 1b, presumably allowing meltwater greater access to the bed. Andersen and others (2010) noted that on Helheim Glacier the velocity response to meltwater production was strongest in heavily crevassed regions close to the front.

Frontal position and calving

The time series of frontal positions shown in Figures 3a and 4a show that the mean calving-front position remained in a stable position from 1985 to 2010, fluctuating by 1.8 km between the most retreated (4 August 2009) and advanced (6 March 2007) positions observed.

Figure 4 includes frontal positions digitized from WSM SAR data and it is easy to identify the occurrence, five or six times a year, of individual cycles of advance and retreat over 0.5–1.0 km. The icebergs seen floating ahead of the calving front in Figure 2 are typical in size and shape for Daugaard Jensen Gletscher and match in width (≥500 m) with the periodic retreats seen in Figure 4. The sawtooth pattern of advance, calving and retreat shown in Figure 4 matches the calving style of a floating ice tongue which emerges as a natural limit of an underlying continuous or discrete fracture process modelled using statistical mechanics (Bassis, 2011). It is more difficult to accurately pinpoint the grounding line than the frontal position for the glacier, but there is no evidence of any change in position throughout the 26 year time series.

It is suggested that the –5°C isotherm for annual mean temperature delimits the minimum latitude of viability for both Antarctic (Vaughan and Doake, 1996) and Greenland (Van der Veen, 2002) ice shelves. The mean annual 2 m air temperature (MAT) at the location of Daugaard Jensen Gletscher's calving front is –5.9°C and it does maintain a short floating ice tongue, identifiable by the 6 km of heavily crevassed surface extending up-glacier from the front. The MAT considered is the 1958–2010 mean of downscaled (to 5 km × 5 km resolution) ECMWF meteorological reanalysis data, corrected for orographic errors in the reanalysis and tuned against surface station temperature data. With the exception of –4.6°C in 1996 all temperatures between 1958 and 2005 were below –5°C, but in 2006 the MAT rose to –1.9°C and has since remained above –2.8°C. If these temperatures persist and the ice-shelf viability limit is indeed

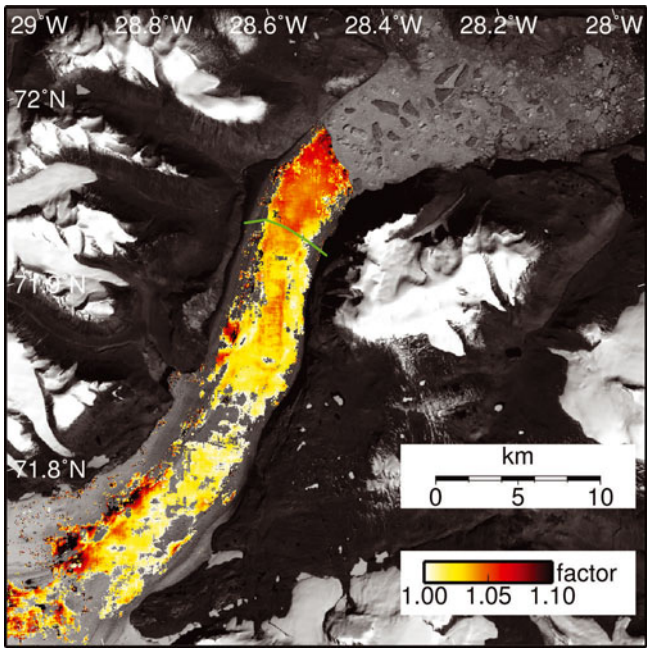

Fig. 5. July acceleration factor based on Landsat-only velocity measurements over the period 1985–2010. The grounding line as identifiable in SAR images (e.g. Fig. 1b) is shown in green.

–5°C, it may be that Daugaard Jensen Gletscher will be unable to support a floating tongue in the future.

The behaviour of Daugaard Jensen Gletscher supports the conclusion that for stable glaciers velocity variations due to changes in terminus position are small compared with meltwater-driven velocity variations (Howat and others, 2010). The onset of summer acceleration is not correlated with any advance/retreat cycle and calving occurs all year round, as can be seen in the WSM frontal position record (Fig. 4). It is more probable that the summer speed-up, which occurs every year, is driven by meltwater penetration to the bed and consequent increases in basal water pressure within an inefficent drainage system allowing enhanced flow.

Mass balance

The modelled 1985–2010 mean annual SMB total for the Daugaard Jensen Gletscher catchment (outlined in Fig. 1) is 9.20 km^3 w.e., with a standard deviation of 2.0 km^3. Stearns and others (2005) used long-term mean accumulation rates for the catchment based on ice-core data (Bales and others, 2001; Zwally and Giovinetto, 2001) to estimate an annual balance flux of 11.4 ± 2.6 km^3 for a point ~45 km further up-glacier. This value agrees, within given errors, with the modelled 1985–2010 mean annual accumulation of 10.65 km^3 (standard deviation 2.0 km^3). Estimated catchment areas also compare well at 48.5×10^3 km^2 (this study) and $50.0 \pm 0.5 \times 10^3$ km^2 (Stearns and others, 2005). Converting the balance flux to a velocity at the grounding line using a mean ice density of 910 kg m^{-3}, a glacier width of 4.6 ± 0.2 km, a thickness of 555 ± 100 m and assuming a rectangular cross section results in a balance velocity of 10.85 m d^{-1}. The glacier width was based on a Landsat image. The thickness was based on the typical observed width of capsized icebergs in the fjord plus 60 m. The 60 m allows for a typical basal melt rate close to the grounding line for north Greenland glaciers of 25 m a^{-1} (Rignot and others, 2001) and a surface melt rate of 5 m a^{-1} (from the modelled rates close to the grounding line) over the ~2 years it takes for ice from the grounding line to reach the calving front.

The error in estimated balance velocity is large: of the order of 35% if the standard deviation of the annual values is used as a measure of the uncertainty in the balance flux. In addition to the estimated errors which may be either positive or negative, the calculated balance velocity is more likely to be an under- than an overestimate of surface velocity at the centre line of a glacier in balance. It is likely to be an underestimate because in converting the balance flux to a surface velocity it was assumed that surface velocities are equal to depth-averaged velocities and that the glacier flows equally fast across the entire width. We also assume that the glacier cross-sectional area is rectangular. It is likely that the depth at the lateral margins is less than that in the centre and that therefore we are overestimating the cross-sectional area.

The measured annual mean surface speed at the grounding line is 8.5 m d^{-1}. This value is a mean of monthly means in order to avoid biasing the value by the greater number of summertime observations. At 10.85 ± 3.8 m d^{-1} the computed balance velocity is greater than the measured annual mean surface speed, which would imply that the glacier should be thickening. This result is not consistent with the observations that the region has apparently been losing mass at a rate of 33.5 ± 6.4 Gt a^{-1} since 2006 (Schrama and Wouters, 2011) and thinning dynamically by 0.3 m a^{-1} during some period between 2002 and 2007 (Pritchard and others, 2009).

The dynamic thinning estimate of 0.3 m a^{-1} (Pritchard and others, 2009) was for a point on the glacier at 2000 m elevation (71.80° N, 30.46° W); at this location the mean modelled SMB for the period 1985–2010 is 0.24 m w.e. Assuming the thinning is due to ice loss, with a density of 910 kg m^{-3}, the ratio of actual flux to balance flux would be given by $[(0.3 \times 0.91) + 0.24]/0.24 = 2.1$. So, given a thinning rate of 0.3 m a^{-1} we would expect actual fluxes to be at least twice as great as balance fluxes. This inconsistency is most probably due to the high uncertainty in the balance velocity stemming from lack of knowledge of glacier geometric parameters such as ice thickness, rather than an underestimate of the annual mean surface speed.

As well as the dynamic stability, annual totals of modelled SMB for the catchment have also been constant, with a standard deviation of only 2% over the period 1985–2010. Therefore, if Daugaard Jensen Gletscher is flowing at rates greater than the balance velocity, and if it is errors in fluxgate geometry, for example, that make it appear otherwise, it must have been doing so for at least the last 26 years and probably for more than 40 years. This would be consistent with the estimate of Hamilton and Whillans (2002) of thinning over a timescale of 100 years based on mean accumulation rates from ice-core data and GPS-based measurements of vertical velocity.

CONCLUSIONS

The successful tracking of surface features in Landsat-5 images has allowed a high temporal resolution time series of surface flow speeds to be reconstructed back to 1985, predating the availability of RADARSAT and ERS data and sampling a climatically cooler period for Greenland (Chylek and others, 2006). In confirmation of earlier studies indicating the dynamic stability of Daugaard Jensen Gletscher from 1968 to 2001 (Stearns and others, 2005) the speed and frontal position data presented here indicate that it continued to be stable through to the end of 2010. A persistent seasonal acceleration of up to 10% occurs over the lower 10 km of the glacier, which is likely to be driven by surface melt onset and not by conditions at the terminus. The front 6 km of the glacier are afloat, and calving occurs all year round, with the location of the front varying by little more than the typical maximum width of calved icebergs. We are unable to detect any imbalance between discharge and SMB, which is at odds with observed elevation decreases (Pritchard and others, 2009) and mass losses (Schrama and Wouters, 2011) for the region. In addition, the observations of dynamic stability described in this paper indicate that if observations of mass loss are accurate and dynamic in origin they must have been present over a multi-decadal time period. This discrepancy between methods of identifying mass balance is not unprecedented for Greenland glaciers and highlights the need for improved observations, particularly of glacier thickness and bed topography. The northerly latitude of Daugaard Jensen Gletscher and its remoteness from the open ocean mean that it has probably not been exposed to the effects of ocean warming which appear to have been driving retreat and flow acceleration of the glaciers farther south on the east coast. However, if the atmospheric warming and observed thinning continue, the grounding line will eventually retreat, calving rates will

increase, the floating tongue will be lost and the glacier will accelerate in a similar manner to glaciers farther south on the east coast.

ACKNOWLEDGEMENTS

We thank the European Space Agency (ESA) for supplying the SAR images, funded by UK Natural Environment Research Council grant NE/G010366/1, and Mark Drinkwater at ESA for facilitating access to the Landsat archive. The ASTER GDEM is a product of the Ministry of Economy, Trade and Industry, Japan (METI) and NASA. Landsat images were also downloaded from the US Geological Survey's Earth Explorer website. The British Atmospheric Data Centre supplied the ECMWF meteorological analysis data. S.L.B. is funded through GLIMPSE, a Leverhulme Trust Research Leadership Scheme project (F/00391/J).

REFERENCES

Amundson JM, Fahnestock M, Truffer M, Brown J, Lüthi MP and Motyka RJ (2010) Ice mélange dynamics and implications for terminus stability, Jakobshavn Isbræ, Greenland. *J. Geophys. Res.,* **115**(F1), F01005 (doi: 10.1029/2009JF001405)

Andersen ML and 14 others (2010) Spatial and temporal melt variability at Helheim Glacier, East Greenland, and its effect on ice dynamics. *J. Geophys. Res.,* **115**(F4), F04041 (doi: 10.1029/2010JF001760)

Bales RC, McConnell JR, Mosley-Thompson E and Csatho B (2001) Accumulation over the Greenland ice sheet from historical and recent records. *J. Geophys. Res.,* **106**(D24), 33 813–33 825 (doi: 10.1029/2001JD900153)

Bales RC and 8 others (2009) Annual accumulation for Greenland updated using ice core data developed during 2000–2006 and analysis of daily coastal meteorological data. *J. Geophys. Res.,* **114**(D6), D06301 (doi: 10.1029/2008JD010600)

Bamber JL, Layberry RL and Gogineni SP (2001) A new ice thickness and bed data set for the Greenland ice sheet. 1. Measurement, data reduction, and errors. *J. Geophys. Res.,* **106**(D24), 33 773–33 780 (doi: 10.1029/2001JD900054)

Bassis JN (2011) The statistical physics of iceberg calving and the emergence of universal calving laws. *J. Glaciol.,* **57**(201), 3–16 (doi: 10.3189/002214311795306745)

Box JE and 8 others (2006) Greenland ice sheet surface mass balance variability (1988–2004) from calibrated polar MM5 output. *J. Climate,* **19**(12), 2783–2800 (doi: 10.1175/JCLI3738.1)

Chen JL, Wilson CR and Tapley BD (2006) Satellite gravity measurements confirm accelerated melting of Greenland ice sheet. *Science,* **313**(5795), 1958–1960 (doi: 10.1126/science.1129007)

Christoffersen P and 7 others (2011) Warming of waters in an East Greenland fjord prior to glacier retreat: mechanisms and connection to large-scale atmospheric conditions. *Cryosphere,* **5**(3), 701–714 (doi: 10.5194/tc-5-701-2011)

Chylek P, Dubey MK and Lesins G (2006) Greenland warming of 1920–1930 and 1995–2005. *Geophys. Res. Lett.,* **33**(11), L11707 (doi: 10.1029/2006GL026510)

Costa-Cabral MC and Burges SJ (1994) Digital elevation model networks (DEMON): a model of flow over hillslopes for computation of contributing and dispersal areas. *Water Resour. Res.,* **30**(6), 1681–1692

Ekholm S (1996) A full coverage, high resolution topographic model of Greenland computed from a variety of digital elevation data. *J. Geophys. Res.,* **101**(B10), 21 961–21 972

Gray L, Short N, Mattar KE and Jezek KC (2001) Velocities and flux of the Filchner Ice Shelf and its tributaries determined from speckle tracking interferometry. *Can. J. Remote Sens.,* **27**(3), 193–206

Hamilton GS and Whillans I (2002) Local rates of ice-sheet thickness change in Greenland. *Ann. Glaciol.,* **35**, 79–83 (doi: 10.3189/172756402781817383)

Hanna E, Huybrechts P, Janssens I, Cappelen J, Steffen K and Stephens A (2005) Runoff and mass balance of the Greenland ice sheet: 1958–2003. *J. Geophys. Res.,* **110**(D13), D13108 (doi: 10.1029/2004JD005641)

Hanna E and 8 others (2008) Increased runoff from melt from the Greenland ice sheet: a response to global warming. *J. Climate,* **21**(2), 331–341

Hanna E, Cappelen J, Fettweis X, Huybrechts P, Luckman A and Ribergaard MH (2009) Hydrologic response of the Greenland ice sheet: the role of oceanographic warming. *Hydrol. Process.,* **23**(1), 7–30 (doi: 10.1002/hyp.7090)

Holland DM, Thomas RH, de Young B, Ribergaard MH and Lyberth B (2008) Acceleration of Jakobshavn Isbræ triggered by warm subsurface ocean waters. *Nature Geosci.,* **1**(10), 659–664 (doi: 10.1038/ngeo316)

Howat IM, Joughin I, Tulaczyk S and Gogineni S (2005) Rapid retreat and acceleration of Helheim Glacier, east Greenland. *Geophys. Res. Lett.,* **32**(22), L22502 (doi: 10.1029/2005GL024737)

Howat IM, Joughin IR and Scambos TA (2007) Rapid changes in ice discharge from Greenland outlet glaciers. *Science,* **315**(5818), 1559–1561 (doi: 10.1126/science.1138478)

Howat IM, Box JE, Ahn Y, Herrington A and McFadden EM (2010) Seasonal variability in the dynamics of marine-terminating outlet glaciers in Greenland. *J. Glaciol.,* **56**(198), 601–613 (doi: 10.3189/002214310793146232)

Janssens I and Huybrechts P (2000) The treatment of meltwater retardation in mass-balance parameterizations of the Greenland ice sheet. *Ann. Glaciol.,* **31**, 133–140 (doi: 10.3189/172756400781819941)

Joughin I, Abdalati W and Fahnestock MA (2004) Large fluctuations in speed on Greenland's Jakobshavn Isbræ glacier. *Nature,* **432**(7017), 608–610 (doi: 10.1038/nature03130)

Joughin I, Das SB, King MA, Smith BE, Howat IM and Moon T (2008) Seasonal speedup along the western flank of the Greenland ice sheet. *Science,* **320**(5877), 781–783 (doi: 10.1126/science.1153288)

Khan SA, Wahr J, Bevis M, Velicogna I and Kendrick E (2010) Spread of ice mass loss into northwest Greenland observed by GRACE and GPS. *Geophys. Res. Lett.,* **37**(6), L06501 (doi: 10.1029/2010GL042460)

Krabill W and 12 others (2004) Greenland ice sheet: increased coastal thinning. *Geophys. Res. Lett.,* **31**(24), L24402 (doi: 10.1029/2004GL021533)

Le Brocq AM, Payne AJ and Siegert MJ (2006) West Antarctic balance calculations: impact of flux-routing algorithm, smoothing algorithm and topography. *Comput. Geosci.,* **32**(10), 1780–1795 (doi: 10.1016/j.cageo.2006.05.003)

Lucchitta BK, Rosanova CE and Mullins KF (1995) Velocities of Pine Island Glacier, West Antarctica, from ERS-1 SAR images. *Ann. Glaciol.,* **21**, 277–283

Luckman A and Murray T (2005) Seasonal variation in velocity before retreat of Jacobshavn Isbræ, Greenland. *Geophys. Res. Lett.,* **32**(8), L08501 (doi: 10.1029/2005GL022519)

Luckman A, Murray T and Strozzi T (2002) Surface flow evolution throughout a glacier surge measured by satellite radar interferometry. *Geophys. Res. Lett.,* **29**(23), 2095 (doi: 10.1029/2001GL014570)

Luckman A, Murray T, Jiskoot H, Pritchard H and Strozzi T (2003) ERS SAR feature-tracking measurement of outlet glacier velocities on a regional scale in East Greenland. *Ann. Glaciol.,* **36**, 129–134 (doi: 10.3189/172756403781816428)

Luckman A, Murray T, de Lange R and Hanna E (2006) Rapid and synchronous ice-dynamic changes in East Greenland. *Geophys. Res. Lett.,* **33**(3), L03503 (doi: 10.1029/2005GL025428)

Luthcke SB and 8 others (2006) Recent Greenland ice mass loss by drainage system from satellite gravity observations. *Science,* **314**(5803), 1286–1289 (doi: 10.1126/science.1130776)

Moon T and Joughin I (2008) Changes in ice front position on Greenland's outlet glaciers from 1992 to 2007. *J. Geophys. Res.,* **113**(F2), F02022 (doi: 10.1029/2007JF000927)

Motyka RJ, Truffer M, Fahnestock M, Mortensen J, Rysgaard S and Howat I (2011) Submarine melting of the 1985 Jakobshavn Isbræ floating tongue and the triggering of the current retreat. *J. Geophys. Res.,* **116**(F1), F01007 (doi: 10.1029/2009JF001632)

Murray T and 10 others (2010) Ocean regulation hypothesis for glacier dynamics in southeast Greenland and implications for ice sheet mass changes. *J. Geophys. Res.,* **115**(F3), F03026 (doi: 10.1029/2009JF001522)

Nick FM, Vieli A, Howat IM and Joughin I (2009) Large-scale changes in Greenland outlet glacier dynamics triggered at the terminus. *Nature Geosci.,* **2**(2), 110–114 (doi: 10.1038/ngeo394)

Pritchard H, Murray T, Luckman A, Strozzi T and Barr S (2005) Glacier surge dynamics of Sortebræ, East Greenland, from synthetic aperture radar feature tracking. *J. Geophys. Res.,* **110**(F3), F03005 (doi: 10.1029/2004JF000233)

Pritchard HD, Arthern RJ, Vaughan DG and Edwards LA (2009) Extensive dynamic thinning on the margins of the Greenland and Antarctic ice sheets. *Nature,* **461**(7266), 971–975 (doi: 10.1038/nature08471)

Reeh N and Olesen OB (1986) Velocity measurements on Daugaard Jensen Gletscher, Scoresby Sund, East Greenland. *Ann. Glaciol.,* **8**, 146–150

Rignot E and Kanagaratnam P (2006) Changes in the velocity structure of the Greenland ice sheet. *Science,* **311**(5673), 986–990 (doi: 10.1126/science.1121381)

Rignot E, Gogineni S, Joughin I and Krabill W (2001) Contribution to the glaciology of northern Greenland from satellite radar interferometry. *J. Geophys. Res.,* **106**(D24), 34 007–34 019

Rignot E, Braaten D, Gogineni P, Krabill WB and McConnell JR (2004) Rapid ice discharge from southeast Greenland glaciers. *Geophys. Res. Lett.,* **31**(10), L10401 (doi: 10.1029/2004GL019474)

Rignot E, Velicogna I, Van den Broeke MR, Monaghan A and Lenaerts J (2011) Acceleration of the contribution of the Greenland and Antarctic ice sheets to sea level rise. *Geophys. Res. Lett.,* **38**(5), L05503 (doi: 10.1029/2011GL046583)

Scambos TA, Dutkiewicz MJ, Wilson JC and Bindschadler RA (1992) Application of image cross-correlation to the measurement of glacier velocity using satellite image data. *Remote Sens. Environ.,* **42**(3), 177–186

Schrama EJO and Wouters B (2011) Revisiting Greenland ice sheet mass loss observed by GRACE. *J. Geophys. Res.,* **116**(B2), B02407 (doi: 10.1029/2009JB006847)

Stearns LA, Hamilton GS and Reeh N (2005) Multi-decadal record of ice dynamics on Daugaard Jensen Gletscher, East Greenland, from satellite imagery and terrestrial measurements. *Ann. Glaciol.,* **42**, 53–58 (doi: 10.3189/172756405781812565)

Strozzi T, Luckman A, Murray T, Wegmuller U and Werner CL (2002) Glacier motion estimation using satellite-radar offset-tracking procedures. *IEEE Trans. Geosci. Remote Sens.,* **40**(11), 2834–2391 (doi: 10.1109/TGRS.2002.805079)

Sundal AV, Shepherd A, Nienow P, Hanna E, Palmer S and Huybrechts P (2009) Evolution of supra-glacial lakes across the Greenland ice sheet. *Remote Sens. Environ.,* **113**(10), 2164–2171 (doi: 10.1016/j.rse.2009.05.018)

Sundal AV, Shepherd A, Nienow P, Hanna E, Palmer S and Huybrechts P (2011) Melt-induced speed-up of Greenland ice sheet offset by efficient subglacial drainage. *Nature,* **469**(7331), 521–524 (doi: 10.1038/nature09740)

Thomas RH and 8 others (2000) Substantial thinning of a major east Greenland outlet glacier. *Geophys. Res. Lett.,* **27** (9), 1291–1294

Van den Broeke M and 8 others (2009) Partitioning recent Greenland mass loss. *Science,* **326**(5955), 984–986 (doi: 10.1126/science.1178176)

Van der Veen CJ (2002) Calving glaciers. *Progr. Phys. Geogr.,* **26**(1), 96–122 (doi: 10.1191/0309133302pp327ra)

Vaughan DG and Doake CSM (1996) Recent atmospheric warming and retreat of ice shelves on the Antarctic Peninsula. *Nature,* **379**(6563), 328–331

Velicogna I (2009) Increasing rates of ice mass loss from the Greenland and Antarctic ice sheets revealed by GRACE. *Geophys. Res. Lett.,* **36**(19), L19503 (doi: 10.1029/2009GL040222)

Velicogna I and Wahr J (2005) Greenland mass balance from GRACE. *Geophys. Res. Lett.,* **32**(18), L18505 (doi: 10.1029/2005GL023955)

Wake L, Huybrechts P, Box JE, Hanna E, Janssens I and Milne GA (2009) Surface mass-balance changes of the Greenland ice sheet since 1866. *Ann. Glaciol.,* **50**(50), 178–184 (doi: 10.3189/172756409787769636)

Wouters B, Chambers D and Schrama EJO (2008) GRACE observes small-scale mass loss in Greenland. *Geophys. Res. Lett.,* **35**(2), L20501 (doi: 10.1029/2008GL034816)

Zwally HJ and Giovinetto MB (2001) Balance mass flux and ice velocity across the equilibrium line in drainage systems of Greenland. *J. Geophys. Res.,* **106**(D24), 33 717–33 728